

Quantum collapse and exponential growth of out-of-time-ordered correlator in anisotropic quantum Rabi model

Shangyun Wang,¹ Songbai Chen,^{2,3,*} Jiliang Jing,^{2,3} Jieci Wang,^{2,†} and Heng Fan⁴

¹*College of Physics and Electronic Engineering, Hengyang Normal University, Hengyang 421002, China*

²*Key Laboratory of Low-Dimensional Quantum Structures and Quantum Control of Ministry of Education, Key Laboratory for Matter Microstructure and Function of Hunan Province, Department of Physics and Synergetic Innovation Center for Quantum Effects and Applications, Hunan Normal University, Changsha 410081, China*

³*Center for Gravitation and Cosmology, College of Physical Science and Technology, Yangzhou University, Yangzhou 225009, People's Republic of China*

⁴*Beijing National Laboratory for Condensed Matter Physics, Institute of Physics, Chinese Academy of Sciences, Beijing 100190, China*

Quantum chaos is an intriguing topic and has attracting a great deal of interests in quantum mechanics and black hole physics. Recently, the exponential growth of out-of-time-ordered correlator (OTOC) has been proposed to diagnose quantum chaos and verify the correspondence principle. Here, we demonstrate that the exponential growth of the OTOC at early times for the initial states centered both in the chaotic and stable regions of the anisotropic quantum Rabi model. We attribute the exponential growth of the OTOC to quantum collapse which provides a novel mechanism of yielding exponential growth of the OTOC in quantum systems. Moreover, the quantum collapse effect is more obvious for the initial states centered in the chaotic one. Our results show that compared with the OTOC, the linear entanglement entropy and Loschmidt echo seem to be more effective to diagnose the signals of quantum chaos in the anisotropic quantum Rabi model.

Introduction—The essential feature of classical chaos is its hypersensitivity to initial conditions, i.e., the so-called butterfly effect. The tiny difference in two nearby orbits grows exponentially with time so that their motions become drastically different. Due to the uncertainty principle, there is no universal quantum counterpart of classical phase-space trajectories, so numerous methods of detecting classical chaos are invalid under quantum circumstances. Thus, it is of fundamental significance to identify the signatures of chaos in a quantum system. In recent years, the OTOC [1] is widely believed to be a powerful tool to detect signatures of chaos in quantum systems because it presents an exponentially growth in time $C(t) \sim e^{\lambda t}$ (where λ is the exponential growth rate of the OTOC before the Ehrenfest time $t_* = \frac{1}{\lambda} \ln N$) as the corresponding classical system is in the chaotic state. Therefore, the OTOC has been used to diagnose the chaotic characteristics in various quantum systems [2–17].

However, besides in the chaotic case, the OTOCs in some non-chaotic regular systems were also found to possess the exponential growth behavior in early time, which means that the exponential growth of the OTOC does not imply the occurrence of chaos in quantum systems. Thus, it is vitally important to study the mechanism of yielding the exponential growth of the OTOC. In the integrable systems, it is shown that quantum mechanics can bring chaos to classical nonchaotic systems [18] and the OTOC at the saddle points grow exponentially [19–21]. Moreover, the exponential growth behavior of OTOCs for unstable regular orbits was found in Ref. [22].

In this letter, we focus on the anisotropic quantum

Rabi model [23, 24], which describes a two-level system coupled to a cavity electromagnetic mode. Recently, due to its well-controlled rotational and antirotational interactions, the anisotropic quantum Rabi model has attracted wide attention ranging from quantum phase transitions [25–28] to quantum state engineering [23, 29]. However, quantum chaos has been rarely studied in the anisotropic quantum Rabi model because it is generally regarded to be far from the so-called thermodynamic limit. If the ratio of the cavity field frequency ω_0 to the atomic transition frequency ω approaches zero, i.e., $\omega_0/\omega \rightarrow 0$, the situation is changed because the truncated photon number N_p of cavity field in this limit tends to infinity, so the system can be regarded as an effective many-body system and the thermodynamic limit [30] can be achieved. On the other hand, the quantum collapse and revival effects have been interpreted theoretically [31–35] and observed experimentally [36–39]. Here, we study the exponential growth of the OTOC in the anisotropic quantum Rabi model and find that quantum collapse provides a new mechanism for the exponential growth of the OTOC.

Model and phase space—The Hamiltonian of the anisotropic quantum Rabi model reads ($\hbar = 1$ hereafter) [23, 24]

$$\begin{aligned} \hat{H} = & \frac{\omega}{2} \sigma_z + \omega_0 a^\dagger a + g_1 (a^\dagger \sigma_- + a \sigma_+) \\ & + g_2 (a^\dagger \sigma_+ + a \sigma_-), \end{aligned} \quad (1)$$

where ω is the atomic transition frequency, $a^\dagger(a)$ is the photonic creation (annihilation) operator of single mode cavity field with frequency ω_0 , g_1 and g_2 are the rotating-wave and counter-rotating-wave coupling

constants, respectively. $\sigma_{\pm} = (\sigma_x \pm i\sigma_y)/2$ and $\sigma_x, \sigma_y, \sigma_z$ are the Pauli matrices.

Here, we take the initial quantum states as

$$|\psi(0)\rangle = |\tau\rangle \otimes |\beta\rangle, \quad (2)$$

with

$$|\tau\rangle = (1 + \tau\tau^*)^{-\frac{1}{2}} e^{\tau\sigma_+} \left| \frac{1}{2}, -\frac{1}{2} \right\rangle, \quad (3)$$

$$|\beta\rangle = e^{-\beta\beta^*/2} e^{\beta a^\dagger} |0\rangle, \quad (4)$$

and

$$\tau = \frac{q_1 + ip_1}{\sqrt{2 - q_1^2 - p_1^2}}, \quad \beta = (q_2 + ip_2)/\sqrt{2}, \quad (5)$$

where $|\tau\rangle$ and $|\beta\rangle$ are Bloch coherent of atom and Glauber coherent states of bosons [40, 41], respectively. The initial quantum states are chosen based on the consideration that their wave packets are minimal in phase space. The states $\left| \frac{1}{2}, -\frac{1}{2} \right\rangle$ and $|0\rangle$ are the ground state of atom and the vacuum state of cavity field, respectively. With the mean field approximation procedure, one can obtain the semiclassical Hamiltonian related to the anisotropic quantum Rabi model,

$$H_{cl} = \frac{\omega}{2}(q_1^2 + p_1^2 - 1) + \frac{\omega_0}{2}(q_2^2 + p_2^2) + \sqrt{1 - (q_1^2 + p_1^2)/2}(G_+q_1q_2 + G_-p_1p_2), \quad (6)$$

where $G_{\pm} = g_1 \pm g_2$, $q_2 = (a^\dagger + a)/\sqrt{2}$ and $p_2 = i(a^\dagger - a)/\sqrt{2}$. With the classical Hamiltonian 6, we obtain

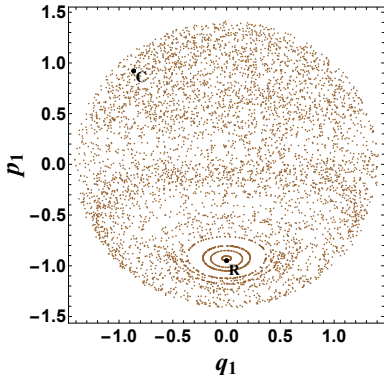


FIG. 1. The Poincaré section for the anisotropic quantum Rabi model in the case: $q_2 = 0, p_2 > 0$, with $\omega = 1, \omega_0 = 0.2, g_1 = 0.9, g_2 = 0.5$ and the system energy $E = 2$. Point $C(q_1 = 0, p_1 = -0.95, q_2 = 0, p_2 = 6.14757)$ and $R(q_1 = -0.86413, p_1 = 0.92136, q_2 = 0, p_2 = 3.37955)$ are situated in chaotic sea and stable island respectively.

a poicaré section of the anisotropic quantum Rabi model, as shown in Fig. 1. It is obvious that there exist the stable regions and the chaotic regions composed of many discrete points. The classical Lyapunov exponent Λ at the initial point C in the chaotic regions is $\Lambda_C \approx 0.134$.

Linear Entanglement entropy—The linear entanglement entropy has been widely used to diagnose chaos in quantum systems [41–43]. It is defined as

$$S(t) = 1 - \text{Tr}_1 \rho_1(t)^2, \quad (7)$$

with the reduced density matrix

$$\rho_1 = \text{Tr}_2 |\psi(t)\rangle\langle\psi(t)|, \quad (8)$$

where Tr_i is a trace over the i th subsystem ($i = 1, 2$) and the wave function $|\psi(t)\rangle$ is the quantum state of the system. Figure 2 shows that the distribution of the time-average entanglement entropy $S_m = \frac{1}{T} \int_{t_1}^{t_2} S(t) dt$ has a good correspondence with classical poicaré section in phase space of Fig. 1, which means that the correspondence principle is applicable to the anisotropic quantum Rabi model. Particularly, there is a significant dip in the time-average entanglement entropy for initial states localized in stable island. The correspondence between the time-average entanglement entropy and the semiclassical phase space not only shows that the entanglement entropy can well diagnose the quantum chaos signal in the anisotropic Rabi model, but also indicates that the classical quantum correspondence can be realized in the system for a single atom interact with cavity field.

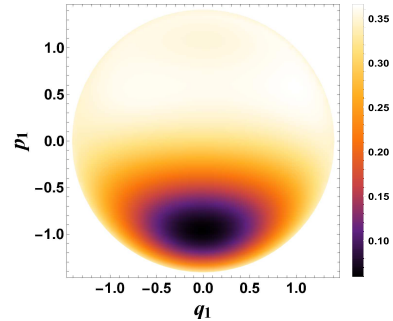


FIG. 2. The distribution of time-average entanglement entropy S_m of Poincaré section in Fig. 1, where the integral interval is $t \in [0, 50]$ and the photon number is truncated at $N_p = 150$.

Loschmidt echo—The Loschmidt echo is another popular way to diagnose the signals of chaos in quantum systems. Considering two Hamiltonians with slight differences acting on the initial state $\psi(0)$, the Loschmidt echo can describe the sensitivity in quantum dynamics similar to the classical dynamics. Let us assume that there exists a constant perturbation δ in the atomic transition frequency in the Hamiltonian, and then the Loschmidt echo can be expressed as

$$L(t) = |\langle\psi(0)|e^{i\hat{H}(\omega)t}e^{-i\hat{H}'(\omega+\delta)t}|\psi(0)\rangle|^2. \quad (9)$$

According to the quantum theory, the overlap of two initial wave functions is supposed to be 1. With the evolution of the two states under the action of two Hamiltonians, the Loschmidt echo decays exponentially for the initial state

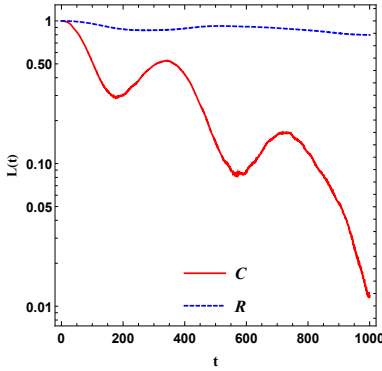


FIG. 3. The Loschmidt echo $L(t)$ is computed for coherent states centered at the chaotic point C and regular point R in Fig. 1. Here, we set $\delta = 0.1$, $\omega = 1$, $\omega_0 = 0.2$, $g_1 = 0.9$, $g_2 = 0.5$ and the photon number is truncated at $N_p = 150$.

centered in the chaotic region, but decays slowly for that in the stable one [44–47]. In Fig. 3, we present the evolution of Loschmidt echo for the initial states centered at the point C (in the chaotic region) and R (in the stable region). Obviously, the Loschmidt echo decays oscillatorily with a larger exponent in the case of the point C , and decays more slowly in the case of the point R . Therefore, the Loschmidt echo clearly identifies the signature of quantum chaos in the anisotropic Rabi model.

Out-of-time-ordered correlator and quantum collapse—Let us now focus on the OTOC, which is another indicator to detect quantum chaos and its form can be defined as [1, 2]

$$C(t) = -\langle [\hat{V}(0), \hat{W}(t)]^2 \rangle, \quad (10)$$

where $\langle \dots \rangle$ denotes the expectation values and $\hat{W}(t) = e^{i\hat{H}t}\hat{W}e^{-i\hat{H}t}$. \hat{H} is a quantum Hamiltonian, \hat{W} and \hat{V} are two approximately local operators [2]. Here, we set $\hat{V} = |\psi\rangle\langle\psi|$ as the projection operator onto the initial state, and the OTOC (10) becomes

$$\text{Var}[\hat{W}(t)] = \langle \psi(t) | \hat{W}^2 | \psi(t) \rangle - \langle \psi(t) | \hat{W} | \psi(t) \rangle^2. \quad (11)$$

Actually, $\text{Var}[\hat{W}(t)]$ is also the quantum variance of operator \hat{W} . Since the wave packet of the cavity field spreads in both directions in phase space, we plot the OTOC (11) as $\text{Var}[q_2(t)] + \text{Var}[p_2(t)]$ for the anisotropic quantum Rabi model with different initial states. As shown in Fig. 4, we find that the OTOC for the system starting from the initial coherent state centered at the point R in Fig. 1 also exhibits an exponential growth behavior, while in its corresponding classical orbit it is stable without exponential growth. For the initial coherent state centered at the point C in the chaotic region, we find that the OTOC of the system still grows exponentially, but its exponential growth rate is greater than the twice of the corresponding

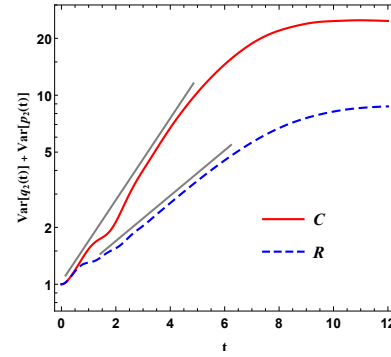


FIG. 4. Time evolution of the OTOC $\text{Var}[q_2(t)] + \text{Var}[p_2(t)]$ for the initial coherent states centered at chaotic point C and regular point R . The gray line is the fitted line and the exponential growth rate of points C and R are $\lambda_C \approx 0.498$ and $\lambda_R \approx 0.276$, respectively. Here, we set $\omega = 1$, $\omega_0 = 0.2$, $g_1 = 0.9$, $g_2 = 0.5$ and the photon number is truncated at $N_p = 150$.

classical Lyapunov exponent, i.e., $\lambda_C > 2\Lambda_C$, which does not satisfy the general relationship between the exponential growth rates of OTOC and classical Lyapunov exponents $\lambda_C = 2\Lambda_C$ [3, 4, 11]. These results indicate that the exponential growth of the OTOC in the anisotropic quantum Rabi model could be caused by other unknown factors besides chaos.

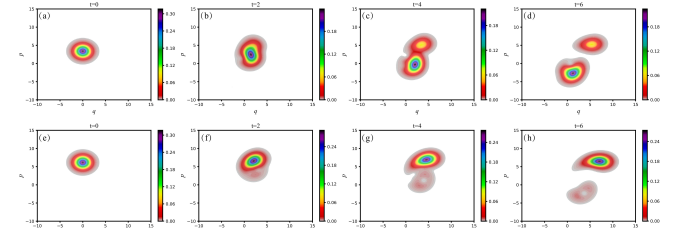


FIG. 5. The time evolution of the Husimi quasi-probabilistic wave packets. The top and bottom panels denote respectively the case in which the initial coherent state centered at the points C and R in Fig. 1. Here, we set $\omega = 1$, $\omega_0 = 0.2$, $g_1 = 0.9$, $g_2 = 0.5$ and the photon number is truncated at $N_p = 150$.

To further unveil the factors yielding the exponential growth of the OTOC, we analyze the evolution of Husimi Q function [48] in the anisotropic quantum Rabi model. The Husimi Q function can provide a visualization of high-dimensional quantum states, demonstrating the dynamical evolution of the quantum state with time. In Fig. 5, we show the evolution of Husimi Q function during the exponential growth of the OTOC for different initial states in the phase space of anisotropic quantum Rabi model. We find that the quantum collapse (the splitting of the wave packet) [35] emerges during the exponential behavior of the OTOC, which does not depend on whether the initial states centered in the chaotic sea or stable island. The

appearance of quantum collapses in both cases is further confirmed by the atomic population inversion with time $W(t)$ as shown in Fig. 6. The atomic population inversion is $W(t) \equiv P_e(t) - P_g(t)$, where $P_e(t)$ and $P_g(t)$ are atomic populations in the excited state $|1/2, 1/2\rangle$ and the ground state $|1/2, -1/2\rangle$, respectively. The non-oscillatory phase of $W(t)$ at early time corresponding to the splitting state of wave packets in quasi-probability distribution in Fig. 5 means that the emergence of quantum collapse of Rabi oscillatory [35]. The split behavior of quantum wave packet in short time implies that the quantum variance of momentum and coordinate operators increase rapidly. This indicates that quantum collapse also gives rise to the exponentially growth behavior of the OTOC in the anisotropic quantum Rabi model. In addition, we find that the quantum collapse effect for the initial coherent state centered in the chaotic sea is more obvious than that in the regular region.

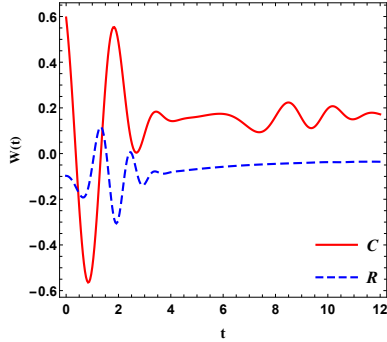


FIG. 6. The evolution of atomic population inversion $W(t)$ for the initial coherent states centered at chaotic point C and regular point R. Here, we set $\omega = 1$, $\omega_0 = 0.2$, $g_1 = 0.9$, $g_2 = 0.5$ and the system energy $E = 2$.

Conclusion— Although the OTOC is generally regarded as a tool of diagnosing quantum chaos, the exponential growth of the OTOC can also be caused by non-chaotic behaviors of quantum systems. Here, we find that quantum collapse can give rise to the exponentially growth behavior of the OTOC in the anisotropic quantum Rabi model, which provides a novel mechanism of yielding exponential growth of the OTOC in quantum systems. Moreover, we show that the classical quantum correspondence can be realized in the anisotropic quantum Rabi model, and both entanglement entropy and Loschmidt echo diagnose quantum chaotic signals effectively in this system.

APPENDIX: OTOC IN JAYNES-CUMMINGS MODEL

In this Appendix, we present the early time growth behavior of the OTOC in the Jaynes-Cummings (JC) model [49]. When the counter-rotating-wave coupling constant $g_2 = 0$, the Hamiltonian 1 and 6 return to

the quantum and classical Hamiltonian of JC model, respectively. In Fig. 7, we exhibit the Poincaré section of JC model. The quasiperiodic orbits on the Poincaré section indicate that the JC model is an integrable system. Moreover, we find that there is no saddle point in the JC model when $\omega = \omega_0 = 1$ and $g_1 = 1$. After excluding quantum instability in the JC model, we also observe the exponential growth behavior of the OTOC in the process of quantum collapse, as shown in Fig. 8. The time to maintain the exponential growth of OTOC coincides well with the time of atomic inversion population oscillation, as seen in the inset of Fig. 8. This further verifies that the quantum collapse leads to the exponential growth of OTOC.

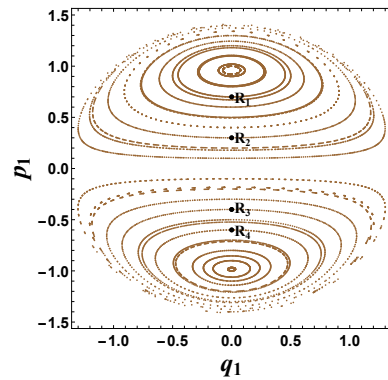


FIG. 7. The Poincaré section for the JC model in the case: $q_2 = 0$, $p_2 > 0$, with $\omega = 1$, $\omega_0 = 1$, $g_1 = 1$ and the system energy $E = 5$. The points R_1 , R_2 , R_3 and R_4 have $q_1 = q_2 = 0$ and mark $(p_1, p_2) = (0.7, 2.69024), (0.3, 3.02284), (-0.4, 3.69836)$ and $(-0.6, 3.85016)$.

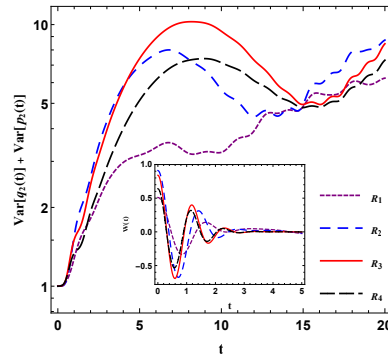


FIG. 8. Time evolution of the OTOC $Var[q_2(t)] + Var[p_2(t)]$ and the atomic population inversion $W(t)$ (see in the inset) for the initial coherent states centered at regular points R_1 , R_2 , R_3 and R_4 in Fig. 7. Here, we set $\omega = 1$, $\omega_0 = 1$, $g_1 = 1$ and the system energy $E = 5$.

* csb3752@hunnu.edu.cn
 † jcwang@hunnu.edu.cn

[1] A. Larkin and Y. Ovchinnikov, Quasiclassical method in the theory of superconductivity, *J. Exp. Theor. Phys.* **28**, 1200 (1969).

[2] D. A. Roberts and D. Stanford, Diagnosing Chaos Using Four Point Functions in Two-Dimensional Conformal Field Theory, *Phys. Rev. Lett.* **115**, 131603 (2015).

[3] J. Maldacena, S. H. Shenker, and D. Stanford, A bound on chaos, *J. High Energy Phys.* **08** (2016) 106.

[4] K. Hashimoto, K. Murata, and Ryosuke Yoshii, Out-of-time-order correlators in quantum mechanics, *J. High Energ. Phys.* **10** (2017) 138.

[5] J. Maldacena and D. Stanford, Remarks on the Sachdev-YeKitaev model, *Phys. Rev. D* **94**, 106002 (2016).

[6] E. B. Rozenbaum, S. Ganeshan, and V. Galitski, Lyapunov Exponent and Out-of-Time-Ordered Correlator's Growth Rate in a Chaotic System, *Phys. Rev. Lett.* **118**, 086801 (2017).

[7] I. García-Mata *et al.*, Chaos Signatures in the Short and Long Time Behavior of the Out-of-Time Ordered Correlator, *Phys. Rev. Lett.* **121**, 210601 (2018).

[8] R. A. Jalabert, I. García-Mata, and D. A. Wisniacki, Semiclassical theory of out-of-time-order correlators for low-dimensional classically chaotic systems, *Phys. Rev. E* **98**, 062218 (2018).

[9] M. McGinley, A. Nunnenkamp, and J. Knolle, Slow Growth of Out-of-Time-Order Correlators and Entanglement Entropy in Integrable Disordered Systems, *Phys. Rev. Lett.* **122**, 020603 (2019).

[10] J. Chávez-Carlos *et al.*, Quantum and Classical Lyapunov Exponents in Atom-Field Interaction Systems, *Phys. Rev. Lett.* **122**, 024101 (2019).

[11] R. J. Lewis-Swan, A. Safavi-Naini, J.J. Bollinger, and A.M. Rey, Unifying scrambling, thermalization and entanglement through measurement of fidelity out-of-time-order correlators in the Dicke model, *Nat Commun* **10**, 1581 (2019).

[12] T. Akutagawa, K. Hashimoto, T. Sasaki and R. Watanabe, Out-of-time-order correlator in coupled harmonic oscillators, *J. High Energy Phys.* **08** (2020) 013.

[13] M. Rautenberg and M. Gärttner, Classical and quantum chaos in a three-mode bosonic system, *Phys. Rev. A* **101**, 053604 (2020).

[14] W. Zhao, Y. Hu, Z. Li, and Q. Wang, Super-exponential growth of out-of-time-ordered correlators, *Phys. Rev. B* **103**, 184311 (2021).

[15] E. R. Castro *et al.*, Quantum-classical correspondence of a system of interacting bosons in a triple-well potential, *Quantum* **5**, 563 (2021).

[16] J. Wang, G. Benenti, G. Casati, and W. Wang, Quantum chaos and the correspondence principle, *Phys. Rev. E* **103**, L030201 (2021).

[17] A. V. Kirkova, D. Porras, and P. A. Ivanov, Out-of-time-order correlator in the quantum Rabi model, *Phys. Rev. A* **105**, 032444 (2022).

[18] E. B. Rozenbaum, L. A. Bunimovich, and V. Galitski, Earlytime exponential instabilities in non-chaotic quantum systems, *Phys. Rev. Lett.* **125**, 014101 (2020).

[19] S. Pilatowsky-Cameo *et al.*, Positive quantum Lyapunov exponents in experimental systems with a regular classical limit, *Phys. Rev. E* **101**, 010202(R) (2020).

[20] T. Xu, T. Scaffidi, and X. Cao, Does Scrambling Equal Chaos?, *Phys. Rev. Lett.* **124**, 140602 (2020).

[21] K. Hashimoto, K. Huh, K. Kimb, and R. Watanabea, Exponential growth of out-of-time-order correlator without chaos: inverted harmonic oscillator, *J. High Energy Phys.* **11** (2020) 068.

[22] S. Wang, S. Chen, J. Jing, Exponential growth of out-of-time-order correlator of regular orbits, *arXiv:2211.10078*.

[23] Q. T. Xie, S. Cui, J. P. Cao, L. G. Amico, and H. Fan, Anisotropic Rabi Model, *Phys. Rev. X* **4**, 021046 (2014).

[24] M. Tomka, O. Araby, M. Pletyukhov, and V. Gritsev, Exceptional and regular spectra of a generalized Rabi model, *Phys. Rev. A* **90**, 063839 (2014).

[25] M.-X. Liu, S. Chesi, Z.-J. Ying, X.-S. Chen, H.-G. Luo, and H.-Q. Lin, Universal Scaling and Critical Exponents of the Anisotropic Quantum Rabi Model, *Phys. Rev. Lett.* **119**, 220601 (2017).

[26] L. T. Shen, Z. B. Yang, H. Z. Wu, and S. B. Zheng, Quantum phase transition and quench dynamics in the anisotropic Rabi model, *Phys. Rev. A* **95**, 013819 (2017).

[27] M.-L. Cai, Z.-D. Liu, W.-D. Zhao, Y.-K. Wu, Q.-X. Mei, Y. Jiang, L. He, X. Zhang, Z.-C. Zhou, and L.-M. Duan, Observation of a quantum phase transition in the quantum Rabi model with a single trapped ion, *Nat. Commun.* **12**, 1126 (2021).

[28] X. Jiang, B. Lu, C. Han, R. Fang, M. Zhao, Zhu Ma, T. Guo, and C. Lee, Universal dynamics of the superradiant phase transition in the anisotropic quantum Rabi model, *Phys. Rev. A* **104**, 043307 (2021).

[29] Y. Y. Zhang and X. Y. Chen, Analytical solutions by squeezing to the anisotropic Rabi model in the nonperturbative deep-strong-coupling regime, *Phys. Rev. A* **96**, 063821 (2017).

[30] L. Bakemeier, A. Alvermann, and H. Fehske, Quantum phase transition in the Dicke model with critical and noncritical entanglement, *Phys. Rev. A* **85**, 043821 (2012).

[31] J. H. Eberly, N. B. Narozhny, and J. J. Sanchez-Mondragon, Periodic Spontaneous Collapse and Revival in a Simple Quantum Model, *Phys. Rev. Lett.* **44**, 1323 (1980).

[32] J. Eiselt and H. Risken, Quasiprobability distributions for the Jaynes-Cummings model with cavity damping, *Phys. Rev. A* **43**, 346 (1991).

[33] C. A. Miller, J. Hilsenbeck, and H. Risken, Asymptotic approximations for the Q function in the Jaynes-Cummings model, *Phys. Rev. A* **46**, 4323 (1992).

[34] A. Alvermann, L. Bakemeier, and H. Fehske, Collapse-revival dynamics and atom-field entanglement in the nonresonant Dicke model, *Phys. Rev. A* **85**, 043803 (2012).

[35] M. Ueda, T. Wakabayashi, and M. Kuwata-Gonokami, Synchronous Collapses and Revivals of Atomic Dipole Fluctuations and Photon Fano Factor beyond the Standard Quantum Limit, *Phys. Rev. Lett.* **76**, 2045 (1996).

[36] G. Rempe, H. Walther, and N. Klein, Observation of quantum collapse and revival in a one-atom maser, *Phys. Rev. Lett.* **58**, 353 (1987).

[37] A. Auffeves *et al.*, Entanglement of a Mesoscopic Field with an Atom Induced by Photon Graining in a Cavity, *Phys. Rev. Lett.* **91**, 230405 (2003).

- [38] D. Lv, S. An, M. Um, J. Zhang, J. Zhang, M. S. Kim, and K. Kim, Reconstruction of the Jaynes-Cummings field state of ionic motion in a harmonic trap, *Phys. Rev. A* **95**, 043813 (2017).
- [39] G. Kirchmair et al, Observation of quantum state collapse and revival due to the single-photon Kerr effect, *Nature (London)* **495**, 205 (2013).
- [40] W. M. Zhang, D. H. Feng, and R. Gilmore, Coherent states: Theory and some applications, *Rev. Mod. Phys.* **62**, 867 (1990).
- [41] K. Furuya, M. C. Nemes, and G. Q. Pellegrino, Quantum Dynamical Manifestation of Chaotic Behavior in the Process of Entanglement, *Phys. Rev. Lett.* **80**, 5534(1998).
- [42] S. Chaudhury, A. Smith, B. E. Anderson, S. Ghose, and P. S. Jessen, Quantum signatures of chaos in a kicked top, *Nature (London)* **461**, 768-771 (2009).
- [43] S. Wang, S. Chen, and J. Jing, Effect of system energy on quantum signatures of chaos in the two-photon Dicke model, *Phys. Rev. E* **100**, 022207 (2019).
- [44] R. A. Jalabert and H. M. Pastawski, Environment-Independent Decoherence Rate in Classically Chaotic Systems, *Phys. Rev. Lett.* **86**, 2490 (2001).
- [45] T. Gorin, T. Prosen, T. H. Seligman, and M. Žnidarič, Dynamics of Loschmidt echoes and fidelity decay, *Phys. Rep.* **435**, **33** (2006).
- [46] Gui-Lei Zhu *et al*, Single-photon-triggered quantum chaos, *Phys. Rev. A* **100**, 023825 (2019).
- [47] A. Bhattacharyya, W. Chemissany, S. S. Haque and B. Yan, Towards the web of quantum chaos diagnostics, *Eur. Phys. J. C* **82**, 87 (2022).
- [48] K. E. Cahill and R. J. Glauber, Density Operators and Quasiprobability Distributions, *Phys. Rev.* **177**, 1882 (1969).
- [49] E. T. Jaynes and F. W. Cummings, Comparison of quantum and semiclassical radiation theories with application to the beam maser, *Proc. IEEE* **51**, 89 (1963).